JOURNAL OF SOLID STATE CHEMISTRY 114, 249–257 (1995)

Tetrahedral-Framework Lithium Zinc Phosphate Phases: Location of Light-Atom Positions in $LiZnPO_4 \cdot H_2O$ by Powder Neutron Diffraction and Structure Determination of $LiZnPO_4$ by *ab Initio* Methods

William T. A. Harrison,*[,1] Thurman E. Gier,† Jacqueline M. Nicol,‡ and Galen D. Stucky†

Department of Chemistry, University of Houston, Houston, Texas 77204-5641; †Department of Chemistry, University of California, Santa Barbara, California 93106-9510; and ‡Reactor Radiation Division, National Institute of Standards and Technology, Gaithersburg, Maryland 20899

Received December 22, 1993; in revised form May 5, 1994; accepted May 7, 1994

The syntheses, crystal structures, and certain properties of two lithium zinc phosphate phases, $LiZnPO_4 \cdot H_2O$ and $LiZnPO_4$, are reported. $LiZnPO_4 \cdot H_2O$ is an isostructure of the Li–*A*-type zeolite $LiAlSiO_4 \cdot H_2O$ and consists of a fully ordered three-dimensional network of vertex-sharing ZnO_4 and PO_4 tetrahedral units surrounding 8-, 6-, and 4-ring windows. The extraframework lithium cation and water molecule are located in this cavity system. These nonframework species (including protons) were unambiguously located by Rietveld refinement against powder neutron data. The structure of $LiZnPO_4$ was solved *ab initio* using synchrotron X-ray powder data and consists of a new "semicondensed" tetrahedral-framework structure, incorporating the guest lithium cations in squashed 6-ring channels. $LiZnPO_4$ may be prepared from $LiZnPO_4 \cdot H_2O$ by a first-order phase transition which involves Zn/P/O bond breaking/making. This transformation is briefly discussed and related to similar transformations in other framework systems. Crystal data: $LiZnPO_4 \cdot H_2O$: $M_r = 185.31$, orthorhombic, space group $Pna2_1$ (No. 33), $a = 10.575(2)$ Å, $b = 8.0759(9)$ Å, $c = 4.9937(6)$ Å, $V = 426.5(2)$ Å^3, $Z = 4$, $T = 15(2)$ K, $R_p = 3.95\%$, $R_{wp} = 5.02\%$, $\chi^2 = 2.33$. $LiZnPO_4$: $M_r = 167.29$, orthorhombic, $Pn2_1a$ (No. 33), $a = 10.0207(2)$ Å, $b = 6.6731(2)$ Å, and $c = 4.96548(8)$ Å, $V = 332.04(2)$ Å^3, $Z = 4$, $T = 298(1)$ K, $R_p = 11.63\%$, $R_{wp} = 15.22\%$, $\chi^2 = 2.82$.

INTRODUCTION

The solid state chemistry of nonaluminosilicate, open-framework materials is currently a very active field of research (1, 2), especially with respect to novel frameworks composed of octahedral *and* tetrahedral subunits (3–5). Aluminophosphates (AlPOs) (6) and gallosilicates (GaSiOs) (7) are now well-established families of molecular sieves with potentially important applications. The crystal chemistry of natural and synthetic beryllophosphates (BePOs) has been explored (8–10). We have shown that the zeolitic behavior of the group (2/12)/(15) (Be/Zn)(P/As)O structure field is extensive (11, 12) and have described several zeolite analogues (13–15) and novel phases (16–18).

Aluminosilicate zeolites, and their structural analogues noted above, often present special crystallographic problems. They are frequently available only as powders, which until recently has precluded the use of "normal" single-crystal structure solution techniques in elucidating zeolite structures. Additionally, the "static" framework/"mobile" guest dichotomy causes problems in experimentation, and in interpretation of diffraction data. The solutions that zeolite crystallographers have developed to overcome these and other problems have been extensively reviewed in a recent article by McCusker (19).

These special crystallographic methods include Rietveld refinements using both X-ray and neutron powder data and *ab initio* structure solution from powder data (20). In this paper we apply these techniques to $LiZnPO_4 \cdot H_2O$ and $LiZnPO_4$, two tetrahedral zincophosphate framework structures, and discuss some aspects of these methods. Both these phases are related to the $LiAlSiO_4 \cdot H_2O$ (Li–*A*, or *ABW*) type aluminosilicate zeolite.

Lithium aluminosilicate zeolite Li–*A* ($LiAlSiO_4 \cdot H_2O$) was structurally characterized by Kerr (21), who found an orthorhombic unit cell, with typical dimensions of $a \approx 10.3$ Å, $b \approx 8.2$ Å, and $c \approx 5.0$ Å, space group $Pna2_1$. Li–*A* consists of infinte stacks of zigzag 4-rings of alternating SiO_4 and AlO_4 tetrahedra, in the polar *c*-unit cell direction. The crosslinking of these stacks results in 6- and 8-ring channels in the *a*- and *c*-unit cell directions respectively, maintaining the alternating, perfect 1 : 1 Si/Al tetrahedral order. The lithium cations are located near the 6-rings and the water molecule occupies the 8-ring channel. Dehydration of H_2O leads to an presumably irre-

[1] To whom correspondence should be addressed.

0022-4596/95 $6.00

versible transformation to other, more condensed phases. Isostructural phases to Li–*A* include the (dehydrated) cesium and rubidium aluminosilicates, $CsAlSiO_4$ and $RbAlSiO_4$, and the nonaluminosilicate lithium gallosilicate ($LiGaSiO_4 \cdot H_2O$) and aluminophosphate *AB*W-type sieves. $LiGaSiO_4 \cdot H_2O$ was the first hydrated zeolite to be fully characterized by powder neutron diffraction methods (22). The *AB*W framework shows considerable flexibility in accomodating the large Cs^+ and Rb^+ cations (23).

SYNTHESIS AND INITIAL CHARACTERIZATION

Powder samples of $LiZnPO_4 \cdot H_2O$ and $LiZnPO_4$ were synthesized during our systematic investigations of the M^+/zinc/phosphate/water (M^+ = Li, Na, K, etc.) structure field, which has produced a number of novel phases (24). A white powder sample of $LiZnPO_4 \cdot H_2O$ was prepared as follows: 7.76 g 2 *M* $Zn(NO_3)_2$ (12 mmol) and 4.79 g 4 *M* H_3PO_4 (16 mmol) were added to a 25-cc Teflon bottle, along with 10 cc H_2O, resulting in a clear solution, to which 11.43 g 4 *M* LiOH (42 mmol) was then added. The bottle was shaken thoroughly, and the initial gel converted to a sludge, and then a milky suspension (pH 5). After 1–2 days at 70°C, the recovered, well-settled powder exhibited a clean orthorhombic Li–*AB*W-type powder pattern (11). White $LiZnPO_4$ powder may be quantitatively prepared from $LiZnPO_4 \cdot H_2O$ powder by a dehydration reaction (100°C in air for 2 days). Alternatively, $LiZnPO_4$ may be synthesized by the direct reaction of $Zn(NO_3)_2$, H_3PO_4, and LiOH solutions, in exactly the same proportions as above, by heat treatment of the resulting sludge at 100°C for 24–48 hr.

The X-ray powder pattern of $LiZnPO_4$ (Scintag automated PAD-X diffractometer, θ–θ geometry, flat plate sample, Cu$K\alpha$ radiation, λ(Cu$K\alpha_1$) = 1.540578 Å, T = 25(2)°C) was indexed on an orthorhombic unit cell, of dimensions a = 10.009(6) Å, b = 6.666(4) Å, and c = 4.957(3) Å (V = 330.7(3) Å^3), and is listed in Table 1. X-ray powder data for $LiZnPO_4 \cdot H_2O$ were listed previously (11).

Powder second-harmonic-generation (PSHG) measurements on $LiZnPO_4$ gave a response of ~14.6 times that of quartz, indicating that $LiZnPO_4$ crystallizes in a noncentrosymmetric space group. Thermogravimetric analysis (TGA) for $LiZnPO_4 \cdot H_2O$ showed ~10 wt% loss between 150–250°C (calc. for complete water loss = 9.7%), and no further weight loss to 500°C. An X-ray powder pattern of the white, post-TGA residue matched that of the monoclinic, high-temperature form of $LiZnPO_4$ (25).

STRUCTURE REFINEMENT FOR $LiZnPO_4 \cdot H_2O$

The crystal structure of the hydrated lithium zincophosphate was refined using powder neutron diffraction data.

TABLE 1
X-Ray Powder Data for $LiZnPO_4$

h	k	l	d_{obs} (Å)	d_{calc} (Å)	Δd^a	$I_{rel}{}^b$
0	1	1	3.976	3.978	−0.001	100
2	1	0	4.003	4.002	0.001	80
1	1	1	3.697	3.696	0.001	17
2	0	1	3.522	3.522	0.000	11
2	1	1	3.114	3.114	0.000	18
2	2	0	2.774	2.774	0.000	30
1	2	1	2.663	2.666	−0.002	18
4	0	0	2.503	2.502	0.001	28
0	0	2	2.479	2.478	0.001	57
2	2	1	2.421	2.421	0.001	17
4	1	0	2.342	2.343	−0.001	7
3	2	1	2.128	2.129	−0.001	13
2	1	2	2.107	2.107	0.000	13
0	3	1	2.029	2.027	0.002	10
3	1	2	1.906	1.906	0.000	9
2	3	1	1.879	1.879	0.000	3
2	2	2	1.847	1.848	−0.001	9
4	0	2	1.761	1.761	0.001	8

[a] $d_{obs} - d_{calc}$.
[b] $100 \times I/I_{max}$.

The very high incoherent neutron scattering cross section of H, leading to a poor signal-to-noise ratio, militates against powder neutron diffraction studies of protonic materials. However, some recent studies (26, 27) have indicated that the crystal structures of relatively simple hydrogenous materials may be studied with neutron powder methods, and the hydrogen-atom positions successfully located and refined.

A pure, well-ground sample of $LiZnPO_4 \cdot H_2O$ was loaded into a 16-mm-diameter vanadium sample can, sealed, and cooled to 15(1) K. Powder neutron data were collected using the diffractometer BT-1 at the National Institute of Standards and Technology, Gaithersburg. A neutron wavelength, calibrated with Al_2O_3 powder, of 1.5454 Å was selected. Data were collected between 5° and 120°, with a step-size of 0.05°, over a 48-hr period, and collated using in-house software into five "banks" covering the ranges 5°–40°, 25°–60°, 45°–80°, 65°–100°, and 85°–120°, respectively.

The Rietveld refinement was carried out using the program GSAS (28) with starting coordinates for the framework species (one Zn, one P, and four O atoms) obtained from the corresponding study (21) of the aluminosilicate Li–*A* phase in space group $Pna2_1$. Coherent neutron scattering factors (in fermis) were assigned as follows: b(Zn) = 0.568, b(P) = 0.513, b(Li) = −0.214, b(O) = 0.581, b(H) = −0.374. After the starting atomic positional and thermal parameters and the usual profile parameters (scale factors, zero-point corrections, polynomial background terms, Gaussian peak shape width-variation

TABLE 2
Crystallographic Parameters

	$LiZnPO_4 \cdot H_2O$	$LiZnPO_4$
Empirical formula	$ZnPO_5LiH_2$	$ZnPO_4Li$
Mol wt.	185.31	167.29
Habit	White powder	White powder
Crystal system	Orthorhombic	Orthorhombic
a (Å)	10.575(2)	10.0207(2)
b (Å)	8.0759(9)	6.6731(2)
c (Å)	4.9937(6)	4.96548(8)
V (Å^3)	426.5(2)	332.04(2)
Z	4	4
Space group	$Pna2_1$ (No. 33)	$Pn2_1a$ (No. 33)
T (K)	15(2)	298(2)
Radiation	Neutrons	X-rays
λ(Å)	1.5454	0.87902
ρ_{calc} (g/cm^3)	2.886	3.346
Number of data	3398	5660
Number of parameters	60	37
R_p[a] (%)	3.95	11.63
R_{wp}[a] (%)	5.02	15.22
χ^2	2.33	2.82

[a] $R_p = \Sigma|y_o - Cy_c|/\Sigma|y_o|$, $R_{wp} = [\Sigma\, w(y_o - C\,y_c)^2/\Sigma w y_o^2]^{1/2}$, where C is a scale factor.

terms, low-angle asymmetry correction, starting lattice parameters from the initial X-ray powder study) and Zn-, P-, and O-atom atomic and thermal parameters were refined to convergence ($R_{wp} \approx 10\%$), the nonframework atoms were progressively located by using difference Fourier syntheses, and added to the refinement. Sites for one oxygen atom, two protons, and one lithium atom were successfully modeled, although bond distance (d(O–H) = 0.95(1) Å) restraints were required to ensure that the proton positions refined to a stable minimum. The refinement converged to final disagreement factors, defined in Table 2, of $R_p = 3.95\%$, $R_{wp} = 5.02\%$, and $\chi^2 = 2.33$. The final observed, calculated and difference profiles for $LiZnPO_4 \cdot H_2O$ are illustrated in Fig. 1.

STRUCTURE DETERMINATION FOR $LiZnPO_4$

The crystal structure of $LiZnPO_4$ was determined *ab initio* from synchroton X-ray powder diffraction data. The X-ray data were collected on the beam line X7a at the Brookhaven National Synchrotron Light Source (NSLS), New York. A thoroughly ground sample of $LiZnPO_4$ was carefully spread over a flat-plate sample holder in air. Room-temperature (25(2)°C) data were collected using a Si(111) channel-cut monochromator and a Ge(220) analyzer crystal at an incident wavelength of 0.87902 Å (calibrated with silicon powder; a = 5.430825 Å at 25(1)°C) with 0.005° step intervals 9° ≤ $2\theta \leq 65°$. The incident beam intensity was monitored with a presample ion chamber and the data were scaled to counts-per-second relative to a nominal 100-mA ring current.

The unit cell was "autoindexed" using the program TREOR (29). Twenty low-angle reflection positions were considered, resulting in a high-figure-of-merit solution with orthorhombic cell constants of $a \approx 10.02$ Å, $b \approx 6.67$ Å, and $c \approx 4.966$ Å. A peak-position simulation in either space group $Pn2_1a$ (nonstandard setting of $Pna2_1$, No. 33) or $Pnma$ (No. 62) accounted for all the observed maxima, giving the reflection conditions $0kl$, $k + l \neq 2n$ absent, and $hk0$, $h \neq 2n$ absent.

Initially, the similarity in unit cells ($a_h \approx a_d$, $b_h \approx 0.75 \times b_d$, $c_h \approx c_d$, of the hydrated (h) and dehydrated (d) lithium zincophosphate materials suggested a close structural relationship between the two phases, presumably via a displacive, non-bond-breaking rearrangement of the framework atoms. However, this is not actually the case in $LiZnPO_4$ (*vide infra*) and efforts at translating the atom positions "on paper" by "squashing" the 8-ring channels and geometric distance-least-squares refinements did not give satisfactory solutions in terms of a reasonable framework geometry, or a satisfactory match to the powder intensities, of the dehydrated phase in either of the space groups mentioned above. Therefore, an *ab initio* structure solution was attempted.

Integrated intensities were extracted from the synchrotron data using the program GSAS, modified according to the method of Le Bail *et al.* (30). The nonstandard space group $Pn2_1a$ was used to maintain the metrical relationship between the unit cell noted above. After careful optimization of the appropriate "profile" parameters (unit-cell parameters, zero-point error, background coefficients, pseudo-Voigt peak shape descriptors) and the intensities themselves, 342 F^2 values having a nonzero intensity, appropriately corrected for Lorentz, polarization, and multiplicity effects, were extracted from the raw data.

The F^2 data were used as the starting data for the direct-methods program SHELXS-86 (31) and a plausible solution for the Zn and P positions was obtained, assuming the material crystallized in the noncentrosymmetric space group $Pn2_1a$. No reasonable starting atomic geometry could be found in space group $Pnma$. Starting positions for the zinc and phosphorus-atom sites were refined and the other atomic species (four oxygen atoms, one lithium atom) were located from difference Fourier maps. The initial refinements were made on the extracted structure factor data using the program CRYSTALS (32). When the model was developed, a Rietveld refinement (program GSAS) against the synchrotron powder X-ray data was carried out. Successful convergence ($R_p = 11.63\%$, $R_{wp} = 15.22\%$, $\chi^2 = 2.82$) was

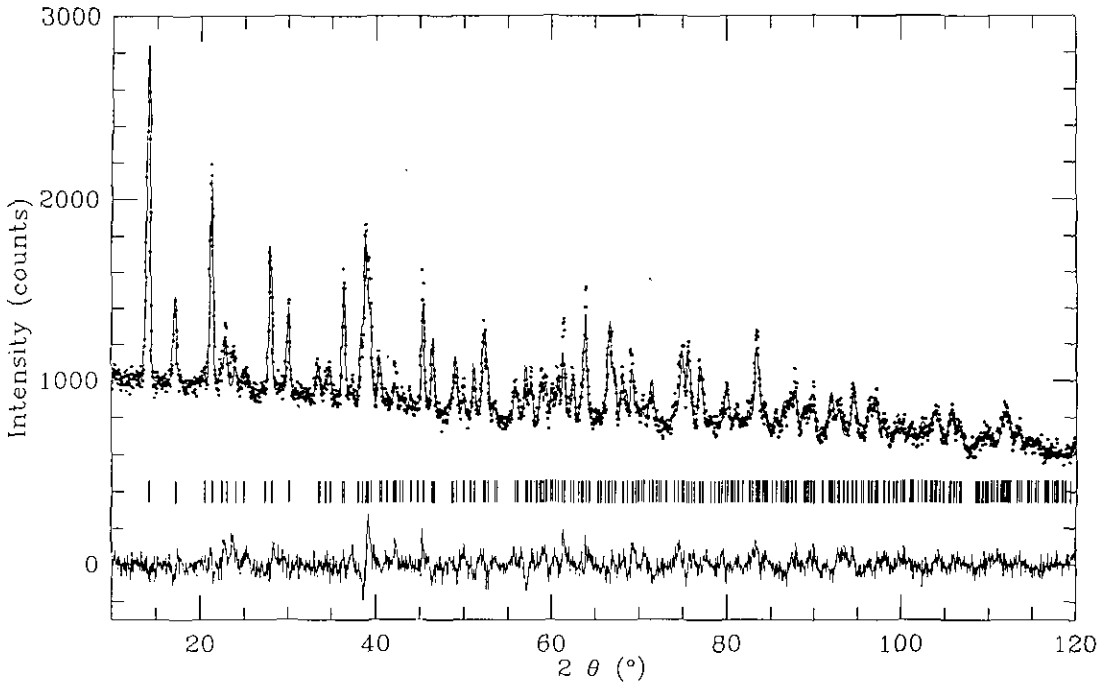

FIG. 1. Final Rietveld observed (dots), calculated (line), and difference profile plots for $LiZnPO_4 \cdot H_2O$, NIST data, λ = 1.5454 Å. Allowed reflection positions are indicated by vertical tick marks. For plotting, the five detector banks were combined into one contiguous profile.

accomplished, and no further reasonable atomic sites could be identified from Fourier maps. Figure 2 shows the final Rietveld plots for $LiZnPO_4$.[2]

CRYSTALLOGRAPHIC RESULTS

Final atomic positional and thermal data for $LiZnPO_4 \cdot H_2O$ are listed in Table 3 with selected bond distances and angles given in Table 4. Similar data for $LiZnPO_4$ are presented in Tables 5 and 6. Both of these phases consist of a three-dimensional network of vertex-linked ZnO_4 and PO_4 tetrahedra, enclosing a network of channels containing the extraframework species described below.

$LiZnPO_4 \cdot H_2O$, whose structure is illustrated in Fig. 3 with ORTEP (33), is confirmed to be isostructural with $LiAlSiO_4 \cdot H_2O$, and contains an alternating, fully ordered array of ZnO_4 and PO_4 groups. Bond distance data (d_{av}(Zn–O) = 1.942(7) Å, d_{av}(P–O) = 1.564(7) Å), which are in accordance with previous structural data for these species in open-framework structures (12, 13, 17), support this assignment. The zinc- and phosphorus-centered tetrahedra are linked via Zn–O–P bonds (θ_{av} = 125.2(5)°) into the three-dimensional *ABW*-type microporous structure. The topology of this structure (Fig. 4) consists of a Zn/P/O framework enclosing 4-, 6-, and 8-ring windows, and is essentially identical to its aluminosilicate analogue which has been exhaustively discussed by Smith (34).

The lithium cation is coordinated by four oxygen atoms, and its location differs in the aluminosilicate and zincophosphate materials. In $LiAlSiO_4 \cdot H_2O$, the lithium cation is statistically disordered over two sites near the 6-ring window, with an apparent Li–Li contact of ~1 Å. In $LiZnPO_4 \cdot H_2O$, just one Li site is occupied, and three Li–O_f bonds (O_f = framework oxygen) are formed, and the fourth Li tetrahedral vertex is to the oxygen atom of the extraframework water molecule (d_{av}(Li–O_f) = 1.93(2) Å). The O–Li–O bond angles around Li are somewhat distorted from those of a regular tetrahedron (min = 88.0, max = 120.9) and a bond valence sum (35) for Li gives 1.08, in good agreement with the expected value of 1.0. This "ordering" of the guest Li cation was also observed in the crystals structure of $LiGaSiO_4 \cdot H_2O$ (22). The water molecule occupies the main 8-ring channels of the structure, as does the oxygen atom of the water molecule in $LiAlSiO_4 \cdot H_2O$. Of the two protons attached to O(5), one, H(1), is involved in an H-bond to a neighboring O(5) atom, with d(O···H) = 1.998(14) Å. The precision of this bond length is overestimated due to the use of O–H

[2] Manufacturers are identified in the above sections in order to provide a complete description of the experimental conditions. This is not intended as an endorsement by the National Institute of Standards and Technology.

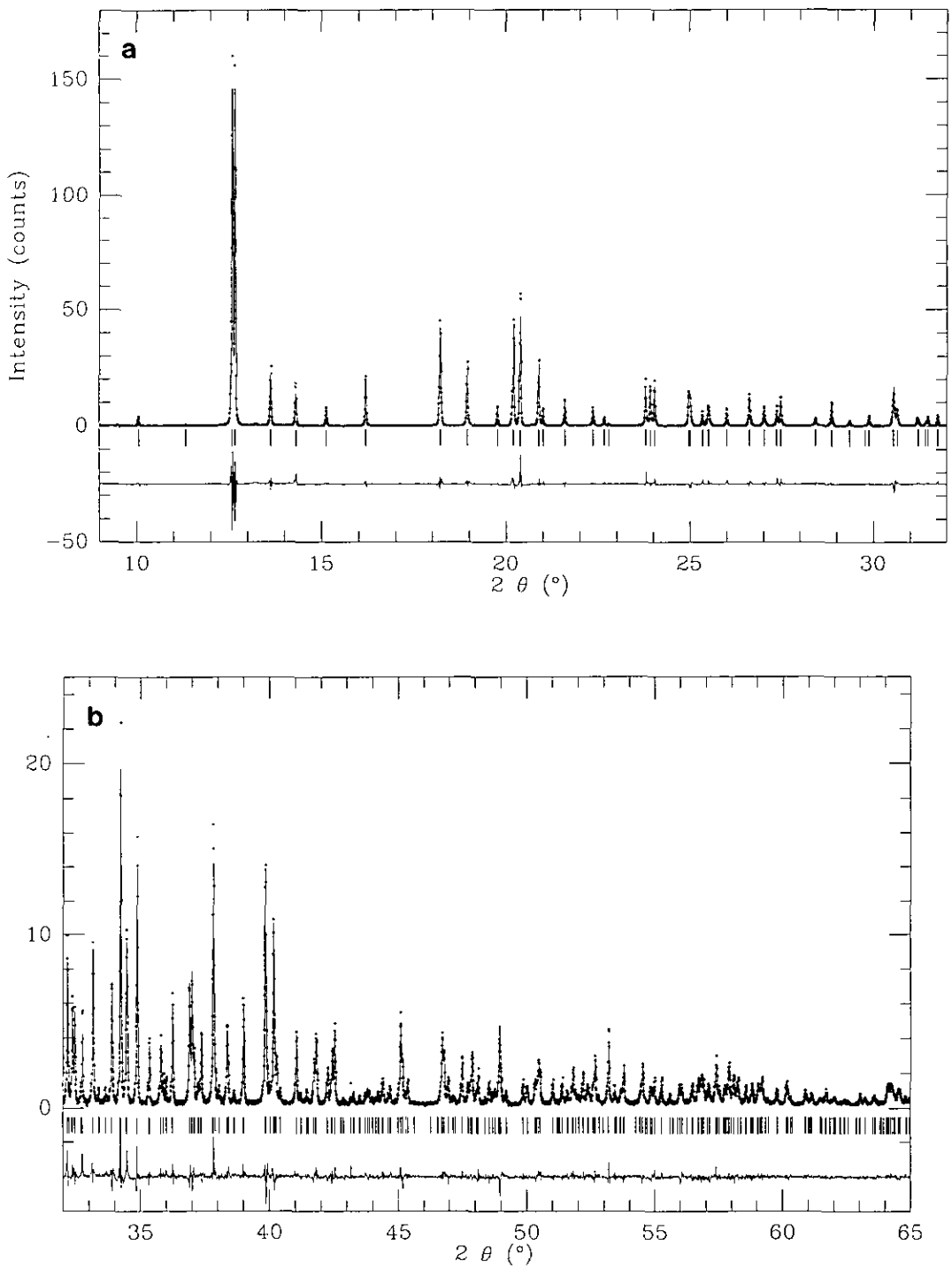

FIG. 2. Final Rietveld observed (dots), calculated (line), and difference profile plots for $LiZnPO_4$, X7a data, $\lambda = 0.87902$ Å. Allowed reflection positions are indicated by vertical tick marks. The profile has been split into two sections to more clearly show the quality of fit at higher angles.

bond-distance restraints mentioned above. H(2) makes no close contacts with other species, apart from its own bound oxygen atom, O(5).

$LiZnPO_4$, whose structure is illustrated with ORTEP in Fig. 5, is a semicondensed phase composed of ZnO_4 and PO_4 subunits, incorporating the tetrahedrally coordinated lithium cations into very distorted, squashed 6-ring channels. One zinc, one phosphorus, one lithium, and four

TABLE 3
Atomic Positional Parameters for $LiZnPO_4 \cdot H_2O$

Atom	x	y	z	$U_{iso}(Å^2)$
Zn(1)	0.1249(10)	0.1064(14)	0.1951(22)	0.011(3)
P(1)	0.3246(9)	0.4117(13)	0.1929(22)	0.011(3)
O(1)	0.9481(8)	0.1618(12)	0.1049(20)	0.008(3)
O(2)	0.2085(9)	0.3152(13)	0.0840(25)	0.008(3)
O(3)	0.1637(10)	0.1052(11)	0.5801(22)	0.008(3)
O(4)	0.1898(11)	0.9331(12)	−0.0026(18)	0.008(3)
Li(1)	0.194(4)	0.311(4)	−0.326(5)	0.032(3)
O(5)	0.5093(12)	0.0920(12)	0.7149(20)	0.032(3)
H(1)	0.4814(18)	0.0595(19)	0.8991(25)	0.032(3)
H(2)	0.4777(20)	0.1920(17)	0.6232(32)	0.032(3)

oxygen atoms make up the asymmetric unit. *All* the oxygen atoms are coordinated to Zn, P, and Li; thus, the phase could equally well be described as being made up from a "framework" of *three* (Zn, P, Li) tetrahedral species rather than just two (Zn and P). The average bond distances of the constituent species are typical: d_{av}(Zn–O) = 1.967(4) Å, d_{av}(P–O) = 1.548(3) Å, d_{av}(Li–O) = 1.96(2)Å. The average Zn–O–P bond angle in $LiZnPO_4$ (119.9(3)°) has decreased by about 5° compared to that found in the hydrated $LiZnPO_4 \cdot H_2O$. The Zn/P/O framework topology (Fig. 6) of $LiZnPO_4$ is composed only from 6-rings of alternating ZnO_4 and PO_4 tetrahedra.

TABLE 4
Bond Distances (Å) and Angles(°) for $LiZnPO_4 \cdot H_2O$

Zn(1)–O(1)	1.974(12)	Zn(1)–O(2)	1.982(16)
Zn(1)–O(3)	1.966(14)	Zn(1)–O(4)	1.845(13)
P(1)–O(1)	1.501(8)	P(1)–O(2)	1.552(16)
P(1)–O(3)	1.666(14)	P(1)–O(4)	1.538(14)
Li(1)–O(2)	2.054(35)	Li(1)–O(3)	1.76(4)
Li(1)–O(4)	1.80(4)	Li(1)–O(5)	2.12(4)
O(5)–H(1)	1.001(9)	O(5)–H(2)	0.987(9)
O(5)···H(1)[a]	1.998(14)		
O(1)–Zn(1)–O(2)	99.5(6)	O(1)–Zn(1)–O(3)	114.9(7)
O(1)–Zn(1)–O(4)	113.7(7)	O(2)–Zn(1)–O(3)	100.7(7)
O(2)–Zn(1)–O(4)	109.2(7)	O(3)–Zn(1)–O(4)	116.2(7)
O(1)–P(1)–O(2)	112.8(8)	O(1)–P(1)–O(3)	101.9(8)
O(1)–P(1)–O(4)	114.8(9)	O(2)–P(1)–O(3)	114.3(8)
O(2)–P(1)–O(4)	109.0(9)	O(3)–P(1)–O(4)	103.7(7)
O(2)–Li(1)–O(3)	107.2(15)	O(2)–Li(1)–O(4)	115.4(20)
O(2)–Li(1)–O(5)	88.0(12)	O(3)–Li(1)–O(4)	120.9(19)
O(3)–Li(1)–O(5)	101.9(20)	O(4)–Li(1)–O(5)	118.2(17)
Zn(1)–O(1)–P(1)	131.9(8)	Zn(1)–O(2)–P(1)	132.9(8)
Zn(1)–O(3)–P(1)	110.6(7)	Zn(1)–O(4)–P(1)	125.3(9)
Zn(1)–O(2)–Li(1)	103.4(11)	Zn(1)–O(3)–Li(1)	107.1(12)
Zn(1)–O(4)–Li(1)	114.0(12)	P(1)–O(2)–Li(1)	114.6(12)
P(1)–O(3)–Li(1)	141.6(14)	P(1)–O(4)–Li(1)	119.3(13)

[a] ··· indicates an H-bonding contact.

DISCUSSION

The utility of powder diffraction methods for the elucidation of subtle structural details has been demonstrated for these lithium zincophosphate materials. Light-atom location in $LiZnPO_4 \cdot H_2O$ was successfully accomplished by using powder neutron diffraction methods, indicating that the Li^+ guest atom in $LiZnPO_4 \cdot H_2O$ occupies a similar site to that found for the Li^+ species in $LiGaSiO_4 \cdot H_2O$ (22), and that the Li^+ species and the extra framework water molecule interact via a Li–O bond, completing the favored tetrahedral coordination of the lithium cation. A

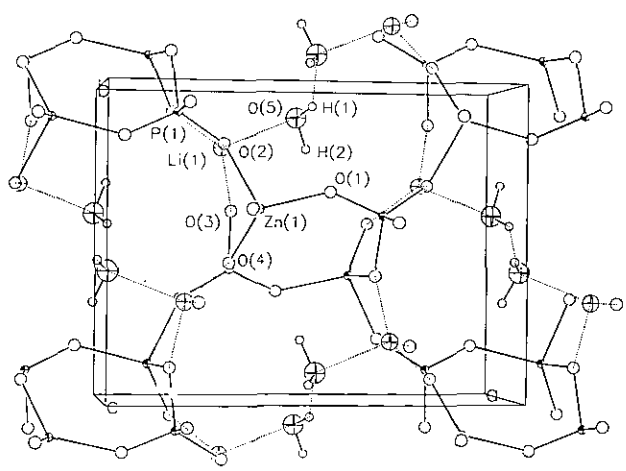

FIG. 3. ORTEP view down the c-direction of the crystal structure of $LiZnPO_4 \cdot H_2O$, with selected atoms labeled. H-bonds and Li–O bonds are indicated by dotted lines.

TABLE 5
Atomic Positional Parameters for $LiZnPO_4$

Atom	x	y	z	$U_{iso}(Å^2)$
Li(1)	0.8507(15)	0.721(7)	0.3088(30)	0.01[a]
Zn(1)	0.34486(11)	0.2127(8)	0.18549(24)	0.019(3)
P(1)	0.40698(23)	0.4613(13)	−0.3160(6)	0.019(3)
O(1)	0.3389(6)	0.2695(15)	−0.2033(12)	0.009(8)
O(2)	0.1593(6)	0.1483(15)	0.3015(12)	0.009(8)
O(3)	0.3847(6)	0.4640(17)	0.3716(12)	0.009(8)
O(4)	0.4432(6)	−0.0358(15)	0.2447(12)	0.009(8)

[a] Not refined.

TABLE 6
Bond Distances(Å) and Angles(°) for $LiZnPO_4$

Zn(1)–O(1)	1.969(6)	Zn(1)–O(2)	1.993(6)
Zn(1)–O(3)	1.956(9)	Zn(1)–O(4)	1.951(8)
P(1)–O(1)	1.554(6)	P(1)–O(2)	1.529(6)
P(1)–O(3)	1.567(6)	P(1)–O(4)	1.542(6)
Li(1)–O(1)	1.998(18)	Li(1)–O(2)	1.997(21)
Li(1)–O(3)	1.96(5)	Li(1)–O(4)	1.89(5)
O(1)–Zn(1)–O(2)	107.26(26)	O(1)–Zn(1)–O(3)	107.72(34)
O(1)–Zn(1)–O(4)	109.07(26)	O(2)–Zn(1)–O(3)	103.82(24)
O(2)–Zn(1)–O(4)	104.15(32)	O(3)–Zn(1)–O(4)	123.66(23)
O(1)–P(1)–O(2)	110.11(33)	O(1)–P(1)–O(3)	107.7(4)
O(1)–P(1)–O(4)	110.8(4)	O(2)–P(1)–O(3)	107.8(4)
O(2)–P(1)–O(4)	109.0(5)	O(3)–P(1)–O(4)	111.44(32)
O(1)–Li(1)–O(2)	104.2(7)	O(1)–Li(1)–O(3)	100.8(14)
O(1)–Li(1)–O(4)	106.9(23)	O(2)–Li(1)–O(3)	103.8(23)
O(2)–Li(1)–O(4)	111.7(15)	O(3)–Li(1)–O(4)	127.0(8)
Zn(1)–O(1)–P(1)	119.9(4)	Zn(1)–O(2)–P(1)	118.1(4)
Zn(1)–O(3)–P(1)	119.1(5)	Zn(1)–O(4)–P(1)	122.5(5)
Zn(1)–O(1)–Li(1)	104.7(6)	Zn(1)–O(2)–Li(1)	105.9(7)
Zn(1)–O(3)–Li(1)	119.8(9)	Zn(1)–O(4)–Li(1)	117.5(10)
P(1)–O(1)–Li(1)	117.2(14)	P(1)–O(2)–Li(1)	123.1(14)
P(1)–O(3)–Li(1)	119.1(10)	P(1)–O(4)–Li(1)	119.9(10)

related "structure-directing" effect has been observed in synthetic lithium beryllophosphate materials, where the Li^+ cation makes three Li–O_f bonds, and a fourth vertex to an extraframework atom. In $LiBePO_4 \cdot H_2O$, this bond is to the oxygen atom of a water molecule, and an *ABW*-type phase is formed (36), similar to $LiZnPO_4 \cdot H_2O$ described here. However, other extraframework entities generate other structures: Cl^- anion leads to a sodalite-type structure, $Li_4Cl(BePO_4)_3$ (37), while HPO_4^{-2} leads to a novel zeolite-*losod*-type network (15).

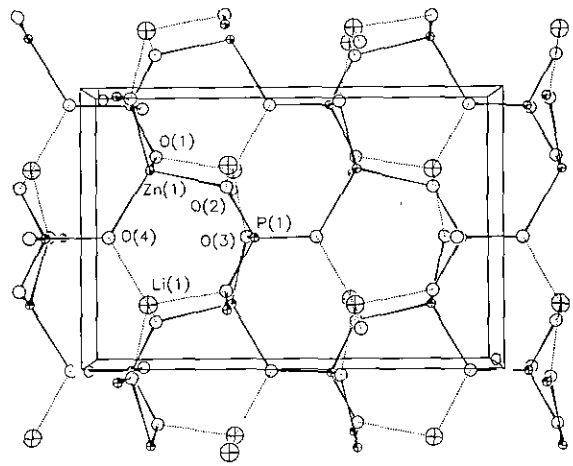

FIG. 5. ORTEP view down the *c*-direction of the crystal structure of $LiZnPO_4$, with selected atoms labeled. Li–O bonds are indicated by *dotted lines*.

The chemical environment of the extraframework water molecule in $LiZnPO_4 \cdot H_2O$ offers insight into the relative importance of *M*–O (*M* = extraframework cation) bonding versus inter-water-molecule or water-molecule-framework H-bonding effects (38). Although water molecules are often disordered or even too mobile to observe by diffraction methods (19), most detailed zeolite crystal-structure studies have indicated that *M*–O bonds are the prime determining factor in water molecule location, and that H-bonds appear to be of secondary importance. In

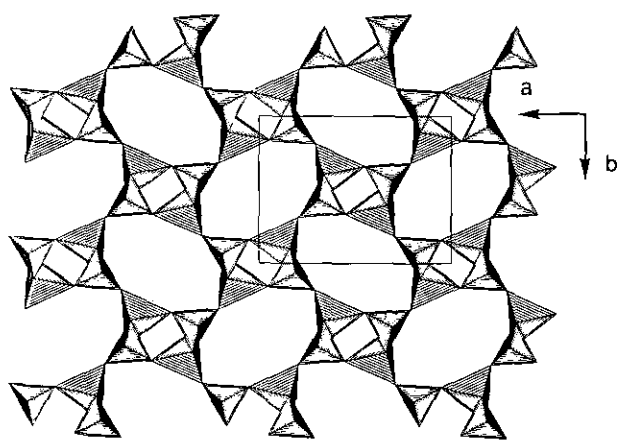

FIG. 4. STRUPLO polyhedral plot (47) of the crystal structure of $LiZnPO_4 \cdot H_2O$, showing the Zn/P/O framework only.

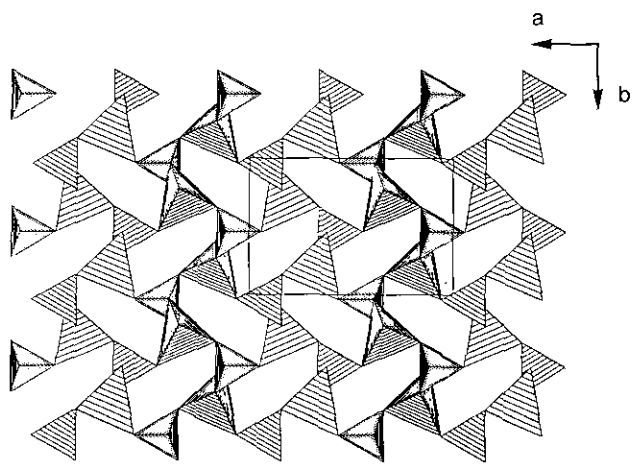

FIG. 6. STRUPLO polyhedral plot of the crystal structure of $LiZnPO_4$, showing the Zn/P/O framework only.

$LiZnPO_4 \cdot H_2O$, the Li-atom tetrahedral-coordination requirement appears to be most significant in determining the O(5)-atom location, although a one-dimensional H-bonding network occurs at the same time, as an infinte chain of O(5)–H(1) $\cdots$ O(5)–H(1) $\cdots$ O(5) ($\cdots$ = H-bond) links (Fig. 3). An analogous situation was observed in $LiGaSiO_4 \cdot H_2O$ (22, 38), where one of the two water-molecule protons hydrogen bonds to a neighboring water-molecule oxygen atom. By comparison, in the sodalite-type $Na_3(ZnAsO_4)_3 \cdot 4H_2O$ (39), one of the extraframework water molecule protons makes an H-bond to a *framework* oxygen atom, indicating that the framework topology is probably most important in determining the various types of extraframework bonding interactions in these phases.

It is notable that upon dehydration, the $LiZnPO_4$ framework has reconstituted from that of $LiZnPO_4 \cdot H_2O$ by Zn–O–P bond breaking/making, and not just by a small geometrical bond distance/angle rearrangement, transforming from a 4-/6-/8-ring network in $LiZnPO_4 \cdot H_2O$ to an all 6-ring topology in $LiZnPO_4$. Framework integrity is usually maintained in aluminosilicate zeolite dehydration reactions (40), but may sometimes cause a rearrangement in aluminophosphate molecular sieve dehydrations (41). In the $LiZnPO_4 \cdot H_2O \rightarrow LiZnPO_4$ process, complete order/alternation of the ZnO_4 and PO_4 species is maintained in each case, although the rearrangement mechanism is unknown at present. This (presumed) first-order phase transformation may be compared to the situation in sodium zincoarsenate sodalite, where a *reversible* dehydration/rehydration reaction transforms $Na_3(ZnAsO_4)_3 \cdot 4H_2O$ (cubic sodalite type, 4-/6-ring topology) to $Na_3(ZnAsO_4)_3$ (hexagonal, all 6-ring topology) (42). Again, ZnO_4 and $(P/As)O_4$ alternating tetrahedral connectivity is preserved, and the Na^+ coordination changes from octahedral in $Na_3(ZnAsO_4)_3 \cdot 4H_2O$ (three framework O + three water-molecule O) to very distorted octahedral (six framework O) in $Na_3(ZnAsO_4)_3$ (42), which is possibly the "driving force" of the reaction.

In $LiZnPO_4$, the reorganized framework may be described as being related to the "stuffed" tridymite-type structure (43), which is the result of one of the particular stacking sequences of different U/D ("up"/"down") combinations of 6-rings of tetrahedra (44). This particular framework has a highly distorted UUUDUD-type configuration, compared to the UDUDUD configuration found in tridymite itself (43). Perhaps the most significant structural feature in $LiZnPO_4$ is the tetrahedral coordination of the Li^+ species in the dehydrated material. This preferred fourfold coordination apparently cannot be attained in the cavities of the dehydrated *ABW*-type network, and greater stability is attained via a framework rearrangement to the all 6-ring $LiZnPO_4$ structure.

It is interesting to note that the crystallographic aspects of the dehydration reaction $LiABO_4 \cdot 4H_2O \rightarrow LiABO_4$ appear to be *different* for *A*, *B* = (Si, Al) or (Si, Ga) and *A*, *B* = Zn, P. The phase $LiAlSiO_4$ exists in several forms (38), but the modification known as δ-eucryptite (38), has unit cell constants of $a \approx 9.90$ Å, $b \approx 6.59$ Å, and $c \approx 4.94$ Å, which are very similar to the lattice constants of $LiZnPO_4$ as described here. However, $LiZnPO_4$ is probably *not* isostructural with δ-$LiAiSiO_4$, nor with lithium gallosilicate, $LiGaSiO_4$, produced in the reaction $LiGaSiO_4 \cdot H_2O \rightarrow LiGaSiO_4$ (38), which shares similar orthorhombic cell constants with $LiZnPO_4$ and $LiAlSiO_4$.

Newsam and Deem, using a novel structure-solution method based on "simulated annealing" (45, 46), determined that the dehydrated $LiGaSiO_4$ structure is based on a 4-/6-/8-ring topology, which may be achieved by a substantial "squashing" of the channel system in $LiGaSiO_4 \cdot H_2O$, as opposed to a possible all 6-ring network, similar to the $LiZnPO_4$ phase described here. Thus, although the structures of $LiZnPO_4$ and $LiGaSiO_4$ are quite different, *their lattice parameters are very similar*, and bear similar relationships to the lattice parameters of their respective hydrated progenitors. However, the space groups of the two types of materials *are* different: the squashed $LiGaSiO_4$ phase crystallizes in space group $Pna2_1$, while the $LiZnPO_4$ phase adopts a structure in $Pn2_1a$, although, coincidentally, these are alternate settings of the same space group. The lithium cation location in the δ-$LiAlSiO_4$ and $LiGaSiO_4$ phases is presently unknown. All the known *ABW* and "dehydrated-*ABW*" phases are summarized in Table 7.

The work described above adds to the growing literature on Group 2/12/15 molecular sieves. The framework

TABLE 7
Summary of Li–*ABW*-Type Unit Cells

Formula	*a* (Å)	*b* (Å)	*c* (Å)	*V* (Å^3)	Reference
$LiBePO_4 \cdot H_2O$	9.662(2)	7.817(2)	4.739(1)	357.9	(36)
$LiBeAsO_4 \cdot H_2O$	10.0408(9)	8.0278(7)	4.8549(5)	391.33	(36)
$LiAlSiO_4 \cdot H_2O$	10.313(1)	8.194(1)	4.993(1)	421.9	(21)
$TlAlSiO_4$	8.297(1)	9.417(1)	5.413(1)	422.9	(49)
$LiZnPO_4 \cdot H_2O$[a]	10.575(2)	8.0759(9)	4.9937(6)	426.5(2)	This work
$RbAlSiO_4$	8.74(1)	9.22(6)	5.33(7)	429.5	(43)
$LiZnPO_4 \cdot H_2O$	10.511(1)	8.1320(9)	5.0273(5)	429.71	(36)
$LiGaSiO_4 \cdot H_2O$	10.461(4)	8.217(4)	5.037(2)	433.0	(38)
$CsAlSiO_4$	8.907(2)	9.435(1)	5.435(1)	456.7	(48)
$LiZnAsO_4 \cdot H_2O$	10.822(2)	8.2913(9)	5.1602(6)	463.02	(36)
$LiAlSiO_4$[b]	9.901(3)	6.594(2)	4.940(1)	322.52	(38, 45)
$LiGaSiO_4$[c]	10.055(3)	6.636(2)	4.968(2)	331.49	(38)
$LiZnPO_4$[d]	10.0207(2)	6.6731(2)	4.96548(8)	332.04(2)	This work

Note. All phases are orthorhombic.
[a] At 15 K.
[b] Condensed 4- /6- /8-ring structure(?).
[c] Condensed 4- /6- /8-ring structure.
[d] Condensed all 6-ring structure.

rearrangement reaction on dehydration of the lithium zincophosphate *ABW* structure versus the framework *distortion* for the lithium aluminosilicate and lithium gallosilicate congeners may offer insight into relative framework stabilities: as previously observed (24), the Group 2/12/15 frameworks tend to be less stable than their aluminosilicate analogues.

ACKNOWLEDGMENTS

We thank Joe Hriljac (Brookhaven National Laboratory) for his assistance with the $LiZnPO_4$ data collection. SHG data were recorded by V. I. Srdanov (*UC* Santa Barbara). This work is partially funded by the National Science Foundation (Division of Materials Research).

REFERENCES

1. R. Szoztak, "Molecular Sieves. Principles of Synthesis and Identification." Van Nostrand, New York, 1989.
2. L. A. Mundi, K. G. Strohmaier, and R. C. Haushalter, *Inorg. Chem.* **30,** 154 (1991).
3. T. Loiseau and G. Férey, *Chem. Commun.* 1197, (1992).
4. S. Feng, M. Tsai, and M. Greenblatt, *Chem. Mater.* **4,** 388 (1992).
5. D. M. Chapman and A. L. Roe, *Zeolites* **10,** 730 (1990).
6. E. M. Flanigen, B. M. Lok, R. L. Patton, and S. T. Wilson, *in* "New Developments in Zeolite Science and Technology." (Y. Murakami, A. Iijima, and J. W. Ward, Eds.), Elsevier, Amsterdam, 1986.
7. J. M. Newsam and D. E. W. Vaughan, *in* "New Developments in Zeolite Science and Technology," (Y. Murakami, A. Iijima, and J. W. Ward, Eds.), Elsevier, Amsterdam, 1986.
8. D. R. Peacor, R. C. Rouse, and J.-H. Ahn, *Am. Mineral.* **72,** 816 (1987).
9. R. C. Rouse, D. R. Peacor, and S. Merlino, *Am. Mineral.* **74,** 1195 (1989).
10. G. Harvey and W. M. Meier, *in* "Zeolites: Facts, Figures, Future" (P. A. Jacobs and R. A. Van Santen, Eds.), Vol. 49, p. 411. Studies in Surface Science and Catalysis, Elsevier, Amsterdam, 1989.
11. T. E. Gier and G. D. Stucky, *Nature (London)* **349,** 508 (1991).
12. W. T. A. Harrison, T. M. Nenoff, T. E. Gier, and G. D. Stucky, *in* "Proceedings 9th International Zeolite Conference, Montreal, 1992" (R. von Ballmoos, J. B. Higgins, and M. M. J. Treacy, Eds.), Vol. I, p. 399. Butterworths, New York, 1993.
13. W. T. A. Harrison, T. E. Gier, K. L. Moran, J. M. Nicol, H. Eckert, and G. D. Stucky, *Chem. Mater.* **3,** 27 (1991).
14. T. M. Nenoff, W. T. A. Harrison, T. E. Gier, and G. D. Stucky, *J. Am. Chem. Soc.* **113,** 378 (1991).
15. W. T. A. Harrison, T. E. Gier, and G. D. Stucky, *Zeolites* **13,** 242 (1993).
16. W. T. A. Harrison, T. E. Gier, and G. D. Stucky, *J. Mater. Chem.* **1,** 153 (1991).
17. W. T. A. Harrison, T. E. Martin, T. E. Gier, and G. D. Stucky, *J. Mater. Chem.* **2,** 175 (1992).
18. W. T. A. Harrison, T. M. Nenoff, M. M. Eddy, T. E. Martin, and G. D. Stucky, *J. Mater. Chem.* **2,** 1127 (1992).
19. L. B. McCusker, *Acta Crystallogr. Sect. A* **47,** 297 (1991).
20. A. K. Cheetham and A. P. Wilkinson, *J. Phys. Chem. Solids* **52,** 1199 (1991).
21. G. T. Kerr, *Z. Kristallogr.* **139,** 186 (1974).
22. J. M. Newsam, *J. Chem. Soc. Chem. Commun.,* 1295 (1986).
23. W. M. Meier and D. H. Olson, "Atlas of Zeolite Structure Types." Butterworth–Heinmann, New York, 1992.
24. T. E. Gier, W. T. A. Harrison, T. M. Nenoff, and G. D. Stucky, *in* "Synthesis of Microporous Materials, Volume I: Molecular Sieves" (M. L. Occelli and H. E. Robson, Eds.), p. 407. Van Nostrand–Reinhold New York, 1992.
25. L. Elammari and B. Elouadi, *Acta Crystallogr. C* **45,** 1864 (1989).
26. A. Le Bail, G. Férey, P. Amoros, and D. Beltran-Porter, *Eur. J. Solid State Inorg. Chem.* **26,** 419 (1989).
27. W. T. A. Harrison, A. V. P. McManus, M. P. Kaminsky, and A. K. Cheetham, *Chem. Mater.* **5,** 1631 (1993).
28. A. C. Larson and R. B. Von Dreele, "GSAS User Guide." Los Alamos National Laboratory, Los Alamos, New Mexico, 1991.
29. P. E. Werner, L. Eriksson, and M. J. Westdahl, *J. Appl. Crystallogr.* **18,** 364 (1987).
30. A. Le Bail, H. Duroy, and J. L. Fourquet, *Mater. Res. Bull.* **23,** 447 (1988).
31. G. M. Sheldrick, "SHELXS-86 User Guide." University of Göttingen, Germany, 1986.
32. D. J. Watkin, J. R. Carruthers, and P. W. Betteridge, "CRYSTALS User Guide." Chemical Crystallography Laboratory, Oxford University, Oxford, UK, 1990.
33. C. K. Johnson, Oak Ridge National Laboratory Report ORNL-5138, with local modifications, Oak Ridge, TN, 1976.
34. J. V. Smith, *Chem. Rev.* **88,** 149 (1988).
35. I. D. Brown and K. K. Wu, *Acta Crystallogr. B* **32,** 1957 (1975).
36. W. T. A. Harrison, T. E. Gier, and G. D. Stucky, unpublished work.
37. T. E. Gier, W. T. A. Harrison, and G. D. Stucky, *Angew. Chem. Int. Ed. Engl.* **30,** 1169 (1991).
38. J. M. Newsam, *J. Phys. Chem.* **92,** 445 (1988).
39. T. M. Nenoff, W. T. A. Harrison, T. E. Gier, N. L. Keder, C. M. Zaremba, V. I. Srdanov, J. M. Nicol, and G. D. Stucky, *Inorg. Chem.* **33,** 2472 (1994).
40. D. W. Breck, "Zeolite Molecular Sieves." Krieger, Malabar, FL, 1984.
41. D. E. Akporiate and M. Stöcker, "Proceedings, 9th International Zeolite Conference, Montreal, 1992" (R. von Ballmoos, J. B. Higgins and M. M. J. Treacy, Eds.), Vol. I, p. 563. Butterworths, New York, 1993.
42. T. M. Nenoff, W. T. A. Harrison, J. M. Newsam, and G. D. Stucky, *Zeolites* **13,** 506 (1993).
43. W. A. Dollase, *Acta Crystallogr. B* **25,** 2298 (1968).
44. R. Klaska and O. Jarchow, *Z. Kristallogr.* **142,** 225 (1975).
45. J. M. Newsam and M. W. Deem, *Nature (London)* **342,** 260 (1989).
46. J. M. Newsam, *in* "Chemistry of Microporous Materials" (T. Inui, S. Namba and T. Tatsumi, Eds.), p. 133. Kodansha, Tokyo, 1991.
47. R. X. Fischer, *J. Appl. Crystallogr.* **18,** 258 (1985).
48. S. A. Gallagher and G. Y. McCarthey, *Mater. Res. Bull.* **12,** 1183 (1977).
49. I. G. Krough-Anderson, E. Krough-Anderson, P. Norby, C. Colella, and M. de'Gennaro, *Zeolites* **11,** 149 (1991).